Electronic Supplementary Material (ESI) for New Journal of Chemistry.

Supporting Information

Microwave Assisted Synthesis of Organically Functionalised Hexa-Molybdovanadates

*Hedi Karoui, Chris Ritchie**

School of Chemistry, University of Melbourne, Parkville, Melbourne, 3010 (Australia)

Table of contents

Materials, Instrumentation and Methods

Chemicals

$(TBA)_4[\beta\text{-}Mo_8O_{26}]$ and $(TBA)_3[H_3V_{10}O_{28}]$ were prepared as previously published.[1] Acetone, acetonitrile, methanol, pentaerythritol, 1,1,1-tris(hydroxymethyl)aminomethane, acetic anhydride, triethylamine and N,N dimethylaminopyridine were reagent grade and used as purchased without any further purification.

Microwave Reactor

Microwave experiments were conducted in a Biotage Initiator Classic, using 2-5 mL reaction vessels.

FT-IR Spectroscopy (KBr disc)

FT-IR spectroscopy was performed using a Bruker Tensor 27 FT-IR spectrometer. Samples were prepared as KBr pellets. Signals are listed as wavenumbers (cm^{-1}) with the following abbreviations: s = strong, m = medium and w = weak.

Elemental Analysis

Elemental Analysis was conducted by the Campbell Microanalytical Laboratory and the Centre for Trace Element Analysis at the University of Otago, New Zealand.

Nuclear Magnetic Resonance (NMR)

^1H NMR spectroscopy was performed on a Varian 400 MHz NMR Spectrometer using a pulse width of π/2 (11.25 μs), carbon decoupled and referenced against residual solvent.

Crystallography

Single crystal X-ray data was collected using an Agilent Technologies SuperNova Dual Wavelength single crystal X-ray diffractometer at 130 K using Cu K-alpha (0.15418 nm) fitted with a mirror monochromator. The data was reduced using CrysAlisPro software (Version 1.171.38.41) using a numerical absorption correction based on Gaussian integration over a multifaceted crystal model. Data was solved using direct methods by SHELXT and refined using a full-matrix least square procedure based upon F^2.[2] Data was refined using the OLEX2 software package Version 1.2.7.[3]

UV-Vis Spectroscopy

UV-Vis spectroscopy was performed on an Agilent Technologies Cary 60 UV-Vis using standard quartz cuvettes (d = 1 cm).

Mass Spectrometry

MS experiments were performed on an Agilent 1100 auto sampler system coupled to an Agilent 6520 Quadrupole Time of Flight (Q-Tof) Mass Spectrometer controlled via the MassHunter software package B.05.01. ESI solutions were prepared using HPLC grade acetonitrile and transferred to the electrospray source. One µl of sample was injected into the carrier solvent stream of 70 % acetonitrile (0.1 % formic acid) at a flow rate of 0.3 mL min^{-1}. Recorded m/z data were corrected using a reference mass by a dual-spray electrospray ionization source using the factory-defined calibration procedure. Mass spectrometer conditions: drying gas flow rate, 7 L $min^{-1;}$ nebulizer pressure, 40 psi; drying gas temperature, 300 °C; capillary voltage, 4000V; skimmer voltage, 65 V; Oct Rf, 750 V; scan range acquired, 100-3200 m/z.

Cyclic Voltammetry

Electrochemical experiments were conducted using a purpose-built cell previously described.[4] All measurements were completed with a 3 mm diameter working; silver-pseudo reference and platinum foil counter electrodes. Tetrabutylammonium hexafluorophosphate was used as supporting electrolyte in freshly degassed acetonitrile. The applied potential was controlled using an Autolab Potentiostat where waveforms were generated using EChem V1.5.2 software in conjunction with a Powerlab 4/20 interface (ADInstruments). All reported cyclic voltammograms are referenced against the ferrocene / ferrocenium redox couple.[5]

Synthesis

$(TBA)_2[V_3Mo_3O_{16}(C_5H_9O_4)]\bullet CH_3CN$ - **1**

$(TBA)_3[H_3V_{10}O_{28}]$ (104 mg, 0.063 mmol), $(TBA)_4[Mo_8O_{26}]$ (166 mg, 0.079 mmol), and pentaerythritol (28 mg, 0.205 mmol) were dissolved in acetonitrile (3 mL) and sealed inside a 5 mL biotage microwave vial. The reaction mixture was heated for 5 minutes at 110 °C, 4 bar. On cooling to room temperature diethyl ether (60 mL) was added while stirring. After 5 minutes the resulting dark red residue was collected and dissolved to make a saturated solution in methanol with crystallization of the product as orange brown plates suitable for x-ray diffraction over the following hours (46 mg, 0.034 mmol, 56 % yield based on vanadium). Elemental analysis $C_{39}H_{84}N_3V_3Mo_3O_{20}$ (MW: 1355.75 g/mol) calculated: C 34.55%, H 6.25%, N 3.1%; found: C 34.66% H 6.41% N 3.25%. Co-crystallization of one acetonitrile solvent molecule.
Selected IR data (KBr, cm^{-1}): 3441(m), 2960(s), 2929(s), 2873(s), 2849(s), 1682(m), 1506(s), 1481(s), 1333(s), 1210(s), 1203(w), 1111(m), 992(s), 810(w), 716(s), 614(m), 500(w), 436(w).

$(TBA)_2[V_3Mo_3O_{16}(C_7H_{11}O_5)]$ **- 2**

Compound **1** (200 mg, 0.16 mmol), acetic anhydride (18 mg, 0.16 mmol), N,N dimethylaminopyridine (DMAP) (8.5 mg, 0.07 mmol) and triethylamine (23 µl, 0.16 mmol) were dissolved in 5 mL CH_3CN and heated at 50 ºC overnight. Solvent was then removed under reduced pressure to yield a dark red residue that was collected and dissolved to make a saturated acetone solution. On diffusion of diethylether into the acetone solution, orange plate crystals suitable for x-ray diffraction formed over 2-5 days. High purity single crystals are collected for further analyses. (20 mg, 0.015 mmol, 11% yield based on vanadium).
Elemental analysis $C_{39}H_{83}N_2V_3Mo_3O_{21}$ (MW: 1354.72 g/mol) calculated: C 34.58%, H 6.17%, N 2.07%; found: C 34.48%, H 6.24%, N 2.27%. Selected IR data (KBr, cm^{-1}): 3441(m), 2960(s), 2929(s), 2873(s), 2849(s), 1730(s), 1628(m), 1481(s), 1461(s), 1383(s), 1318(s), 1220(s), 1201(m), 1131(s), 992(s), 801(s), 716(s), 614(m), 500(w), 436(w).

$(TBA)_2[V_3Mo_3O_{16}(C_4H_8NO_3)]\bullet CH_3CN$ **- 3**

$(TBA)_3[H_3V_{10}O_{28}]$ (104 mg, 0.063 mmol), $(TBA)_4[Mo_8O_{26}]$ (166 mg, 0.079 mmol) and 1,1,1-tris(hydroxymethyl)aminomethane (25 mg, 0.205 mmol) were dissolved in acetonitrile (3 mL) and sealed inside a 5 mL biotage microwave vial. The reaction mixture was heated for 5 minutes at 110 °C, 4 bar. On cooling to room temperature diethyl ether (60 mL) was added while stirring. After 5 minutes the resulting dark red residue was collected by centrifugation. This procedure was repeated 4 times until a thick red oil is obtained. The red oil was then dissolved in 5 mL acetonitrile/dimethylformamide (10:1), with red-orange crystals forming on slow evaporation of the solvent. (35 mg, 0.026 mmol, 43 % yield based on vanadium).

$C_{38}H_{83}N_4V_3Mo_3O_{19}$ (MW: 1340.74 g/mol) calculated: C 34.04%, H 6.24%, N 4.18%; found: C 34.72%, H 6.77%, N 3.41%. Co-crystallization of one acetonitrile solvent molecule.
Selected IR data (KBr, cm^{-1}): 3441(m), 2960(s), 2929(s), 2873(s), 2849(s), 1750(w), 1680(w), 1515(s), 1481(s), 1220(w), 1131(s), 992(s), 952(s), 883(m), 801(s), 716(s), 614(m), 500(m), 436(m).

Nuclear Magnetic Resonance (NMR)

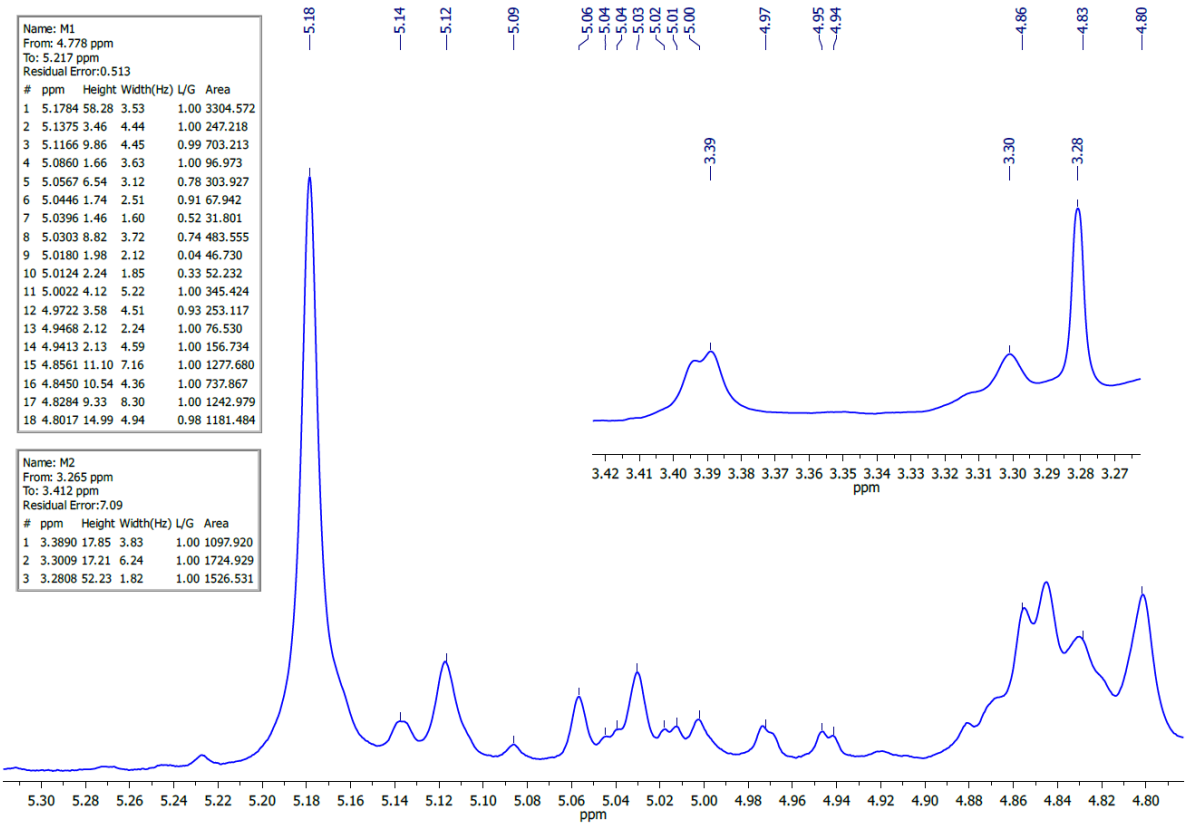

Figure S1. ^{1}H NMR (D_3-CD_3CN) of a freshly dissolved sample of **1**.

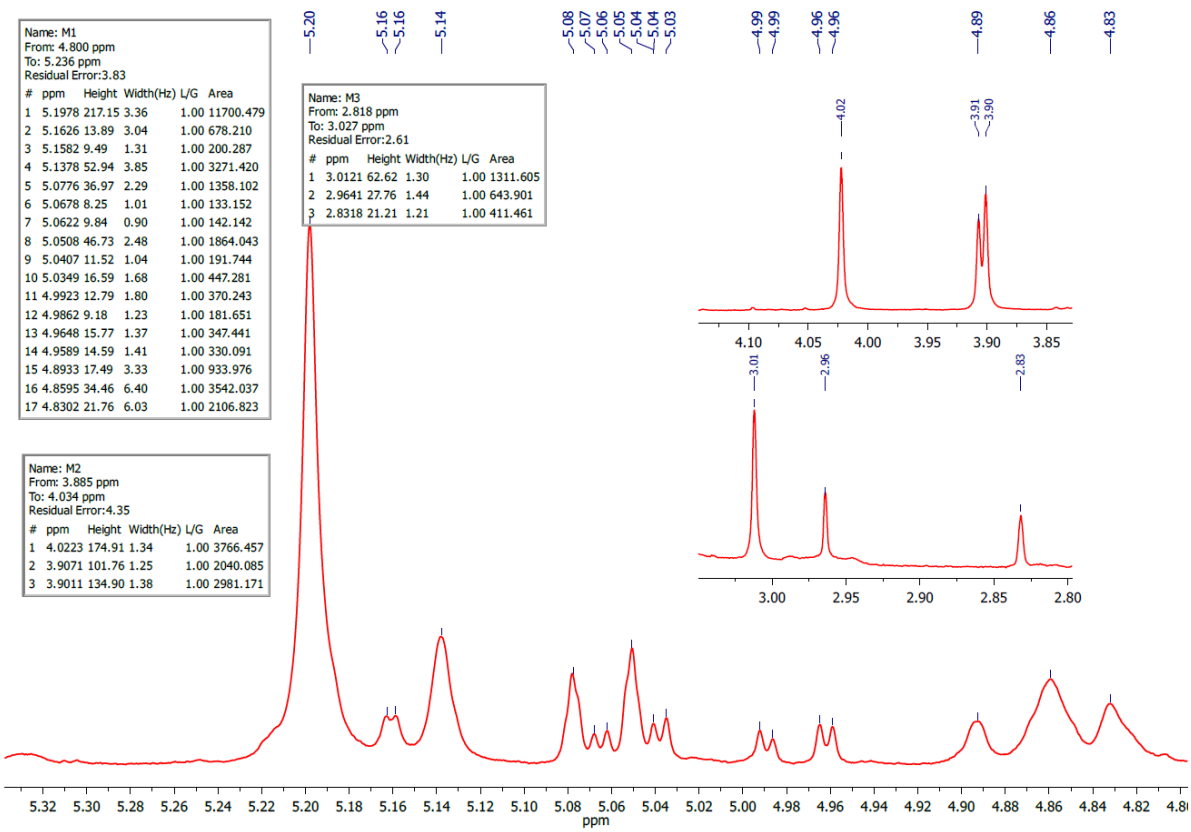

Figure S2. ^{1}H NMR (D_3-CD_3CN) of a freshly dissolved sample of **2**.

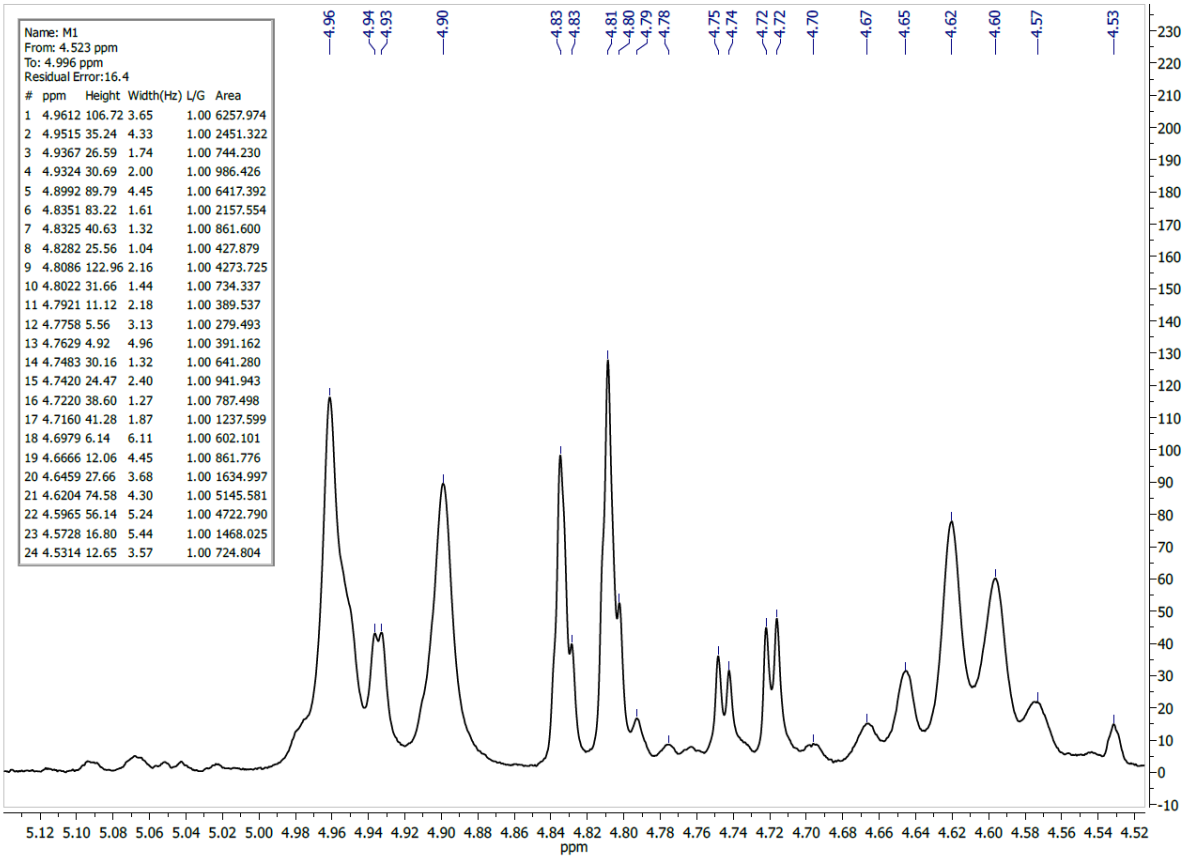

Figure S3. ^{1}H NMR (D_3-CD_3CN) of a freshly dissolved sample of **3**.

Infrared Spectroscopy

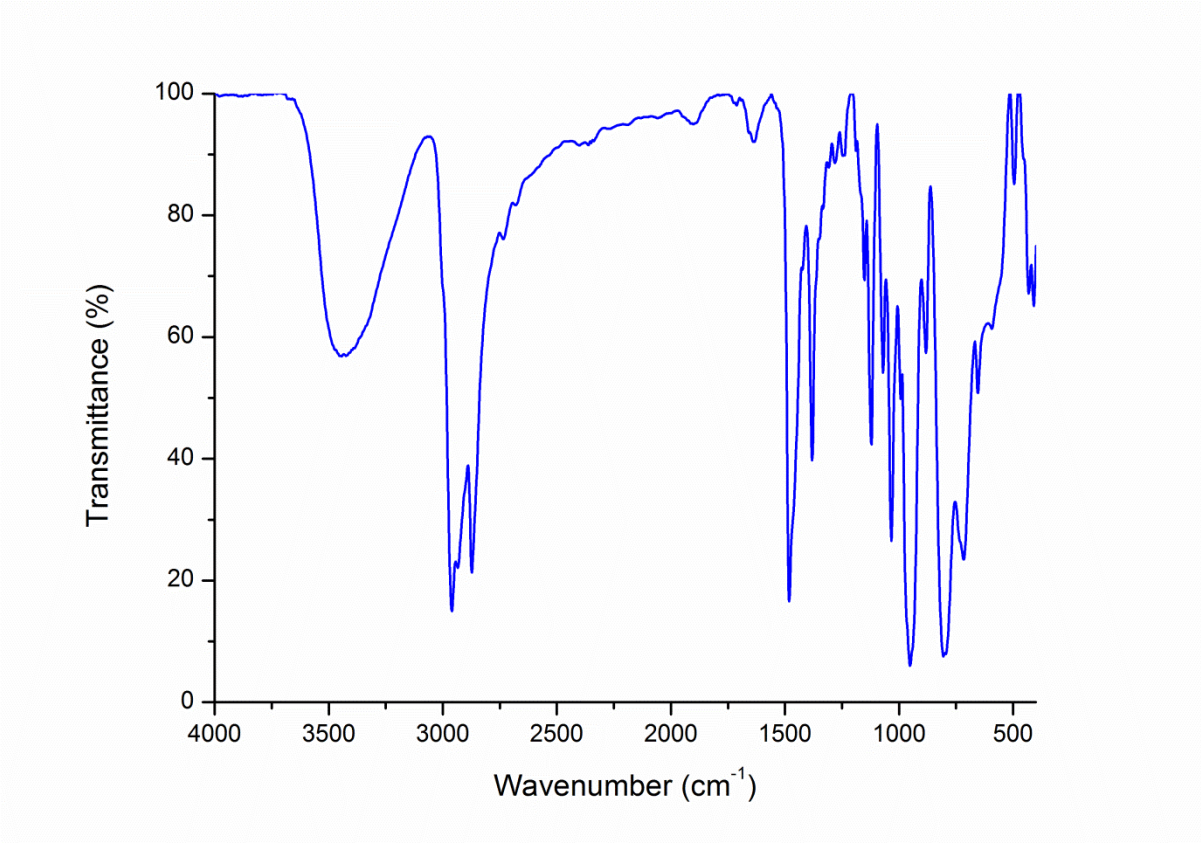

Figure S4. Infrared spectrum of a freshly crystallised sample of **1**.

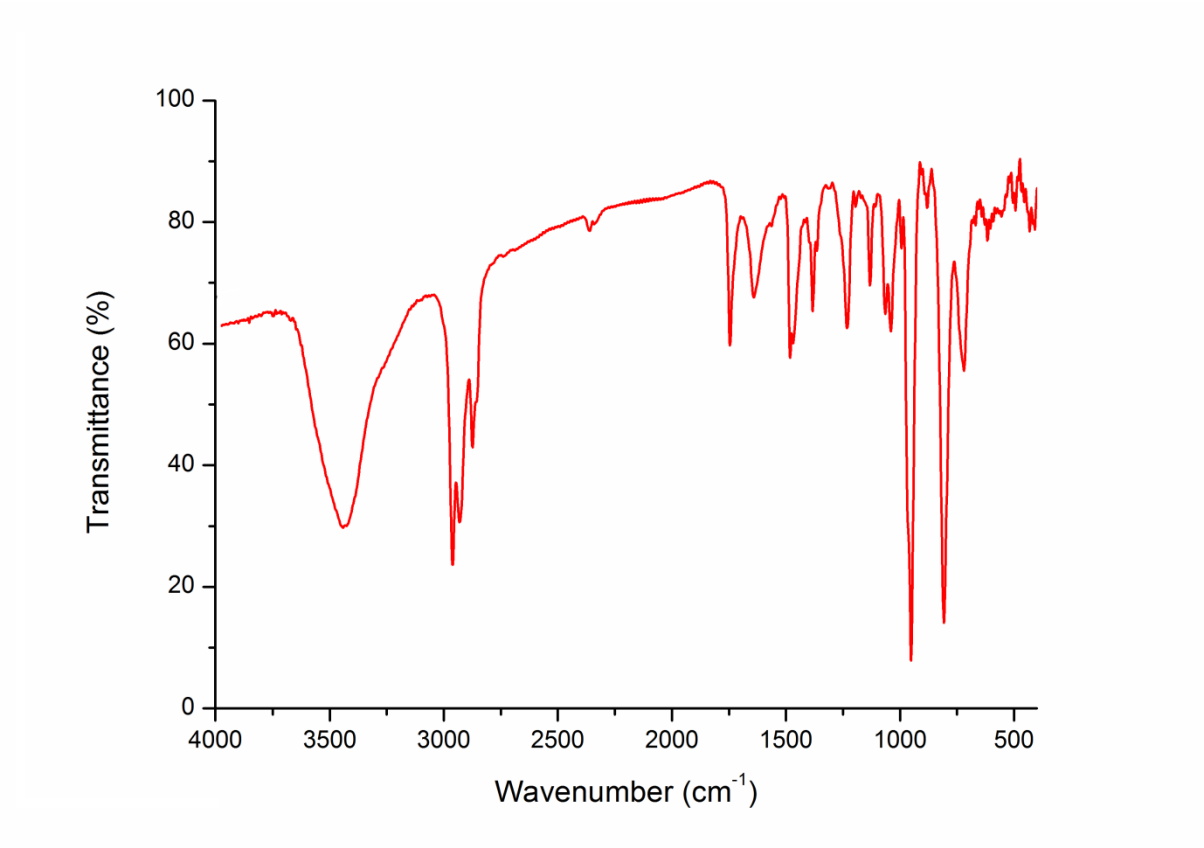

Figure S5. Infrared spectrum of a freshly crystallised sample of **2**.

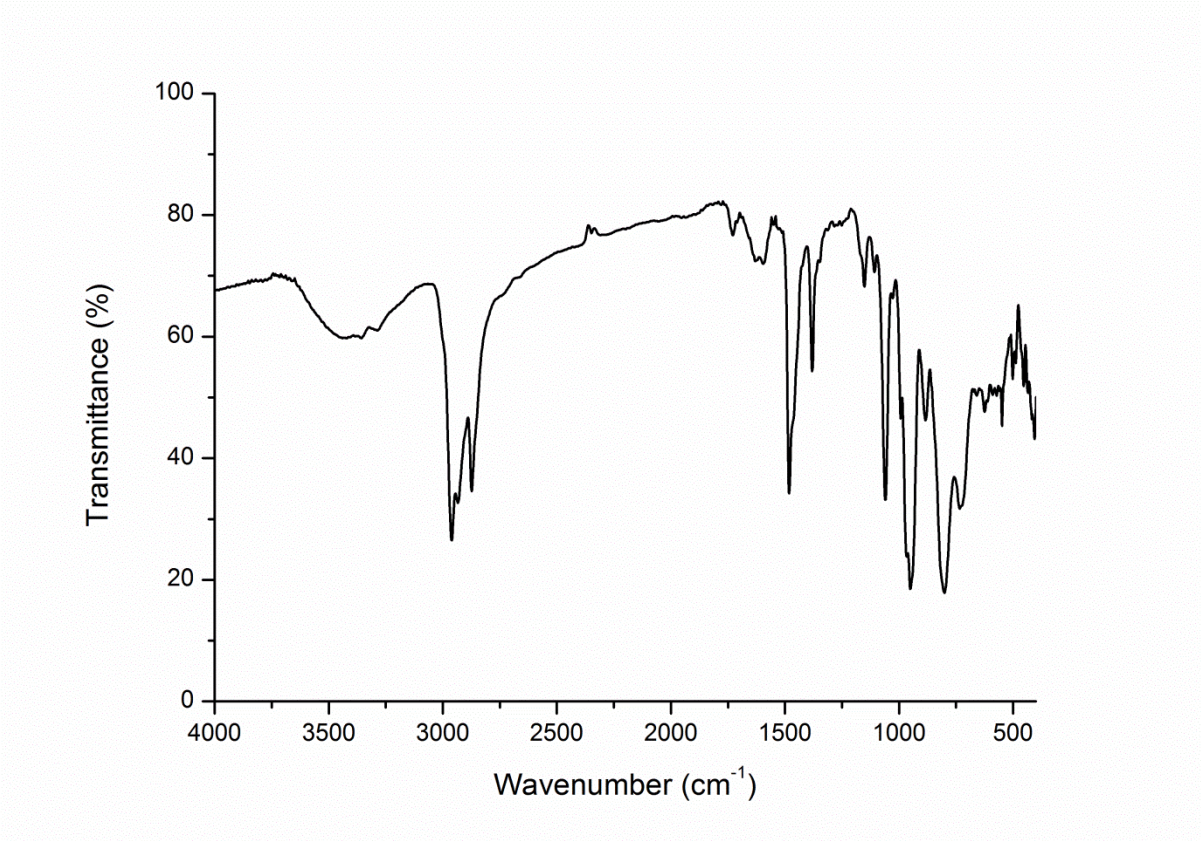

Figure S6. Infrared spectrum of a freshly crystallised sample of **3**.

UV-Vis Spectroscopy

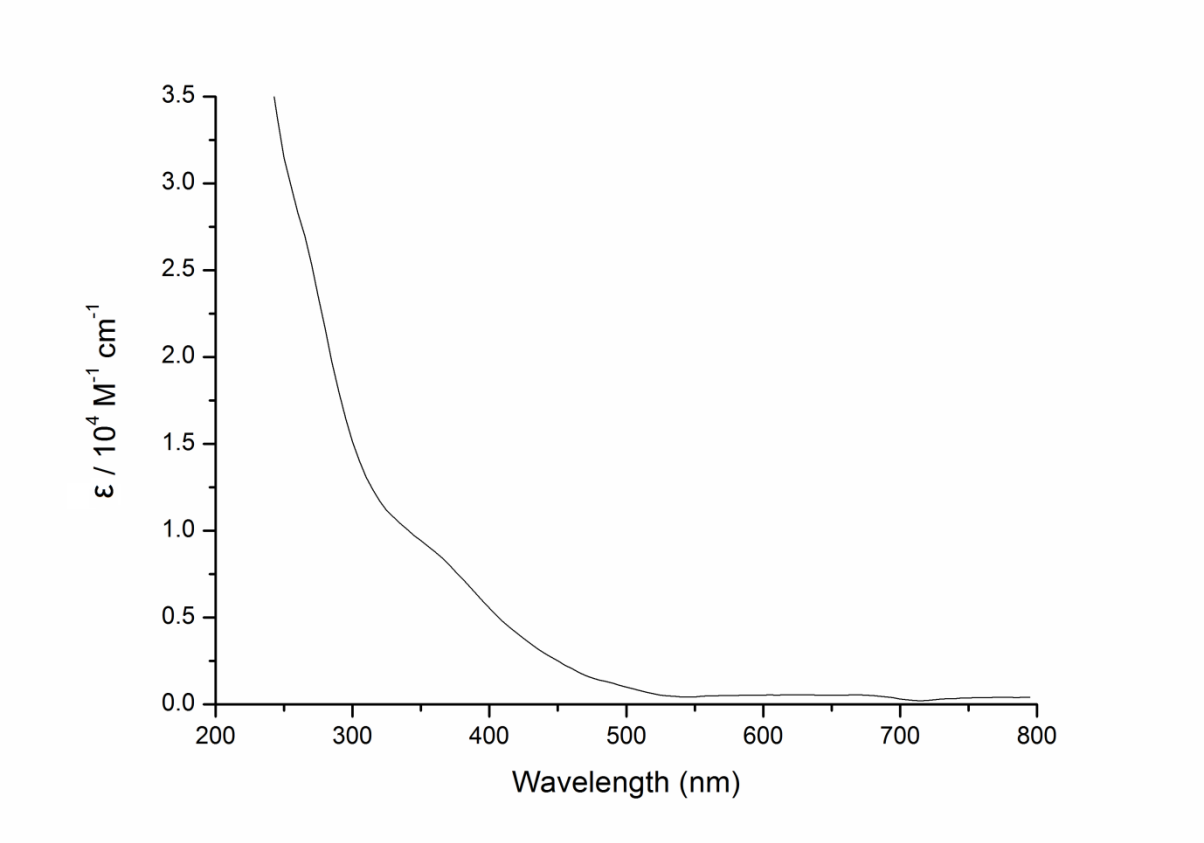

Figure S7. UV-Vis spectrum of a freshly dissolved sample of **1** (0.08 mM) in acetonitrile. λmax_1 = 365 nm, ε = 0.882× 10^4 M^{-1} cm^{-1}; λmax_2 = 270 nm, ε = 2.540 × 10^4 M^{-1} cm^{-1}.

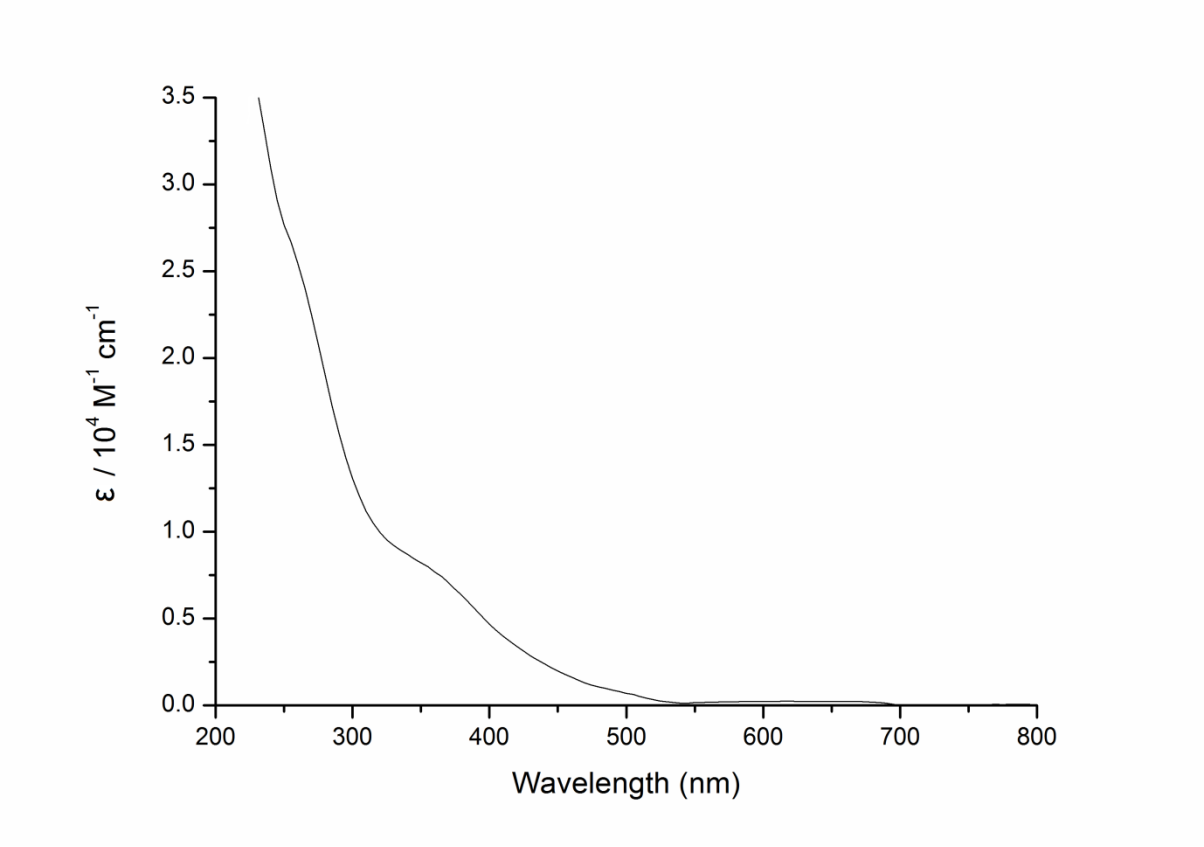

Figure S8. UV-Vis spectrum of a freshly dissolved sample of **2** (0.08 mM) in acetonitrile. λmax_1 = 365 nm, ε = 0.767 × 10^4 M^{-1} cm^{-1}; λmax_2 = 270 nm, ε = 2.236× 10^4 M^{-1} cm^{-1}.

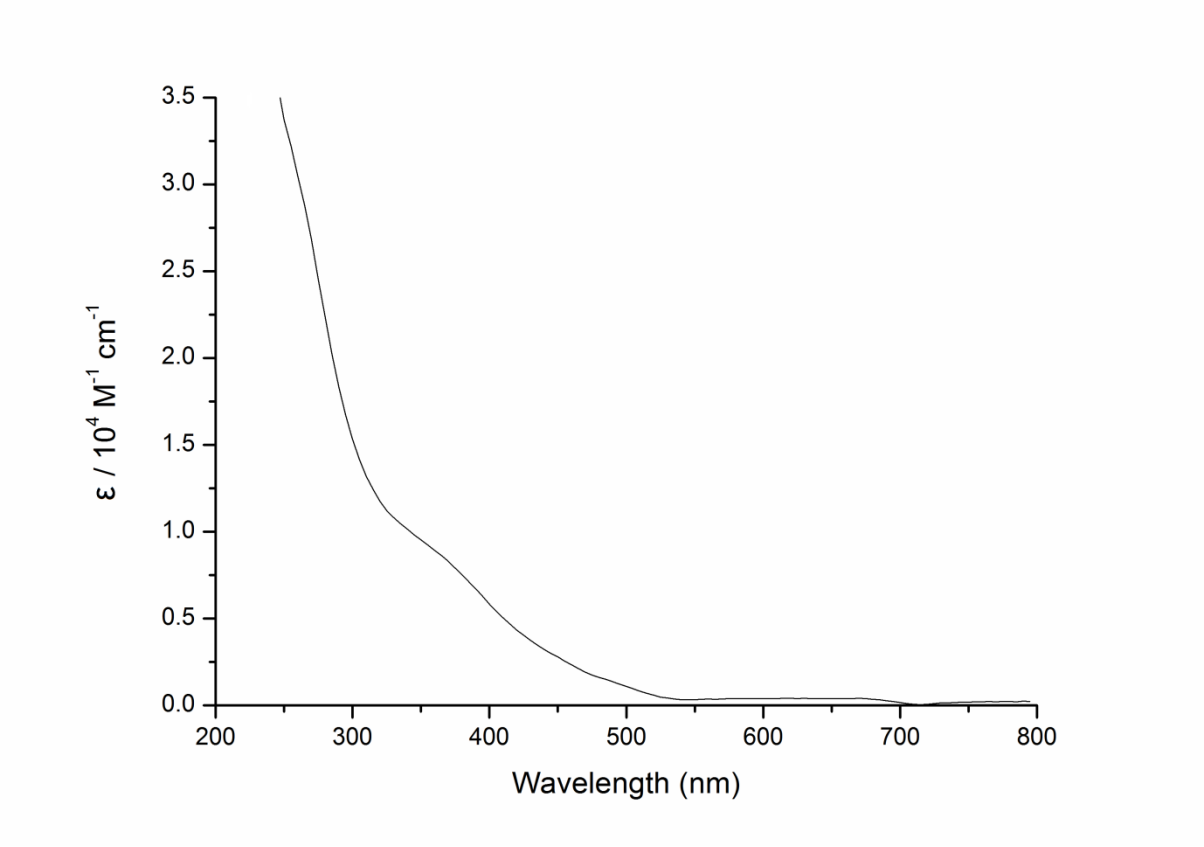

Figure S9. UV-Vis spectrum of a freshly dissolved sample of **3** (0.08 mM) in acetonitrile. λmax_1 = 365 nm, $\varepsilon = 0.899 \times 10^4$ M^{-1} cm^{-1}; λmax_2 = 270 nm, $\varepsilon = 2.688 \times 10^4$ M^{-1} cm^{-1}.

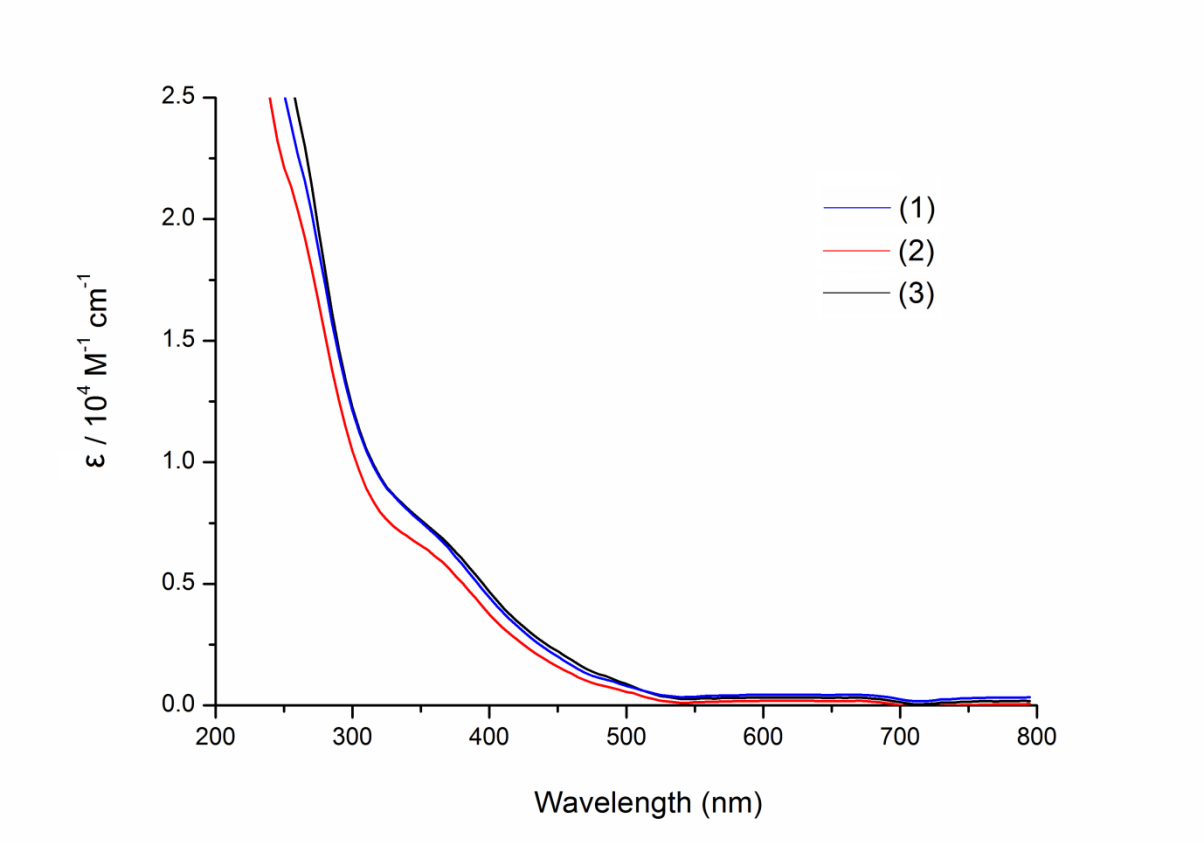

Figure S10. UV-Vis spectrum of a freshly dissolved sample of **1-3** (0.08 mM) in acetonitrile.

High Resolution Electrospray Ionization Mass Spectrometry

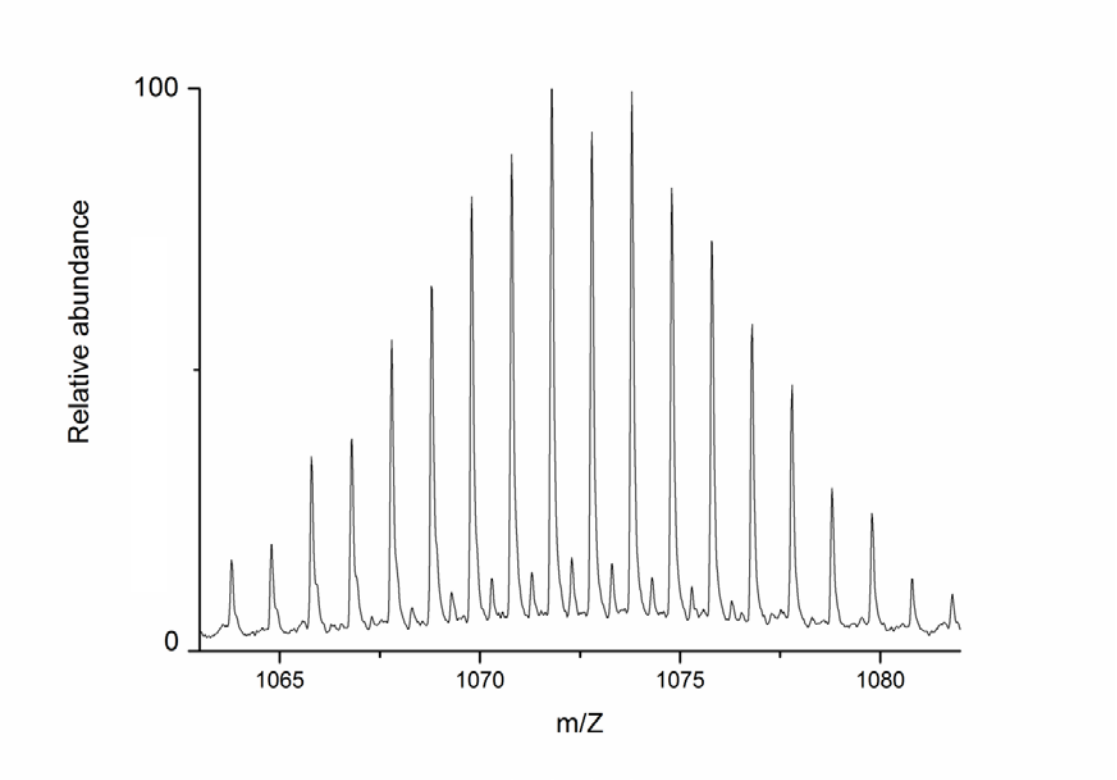

Figure S11. HRMS spectrum of **1** representing the isotopic pattern of TBA$[V_3Mo_3O_{16}(C_5H_9O_4)]^{1-}$.

Table S1. Assignment of HRMS of **1** in the negative ion mode.

Peak (m / z)	Assignment
1072 Da	TBA$[V_3Mo_3O_{16}(C_5H_9O_4)]^{1-}$
415 Da	$[V_3Mo_3O_{16}(C_5H_9O_4)]^{2-}$

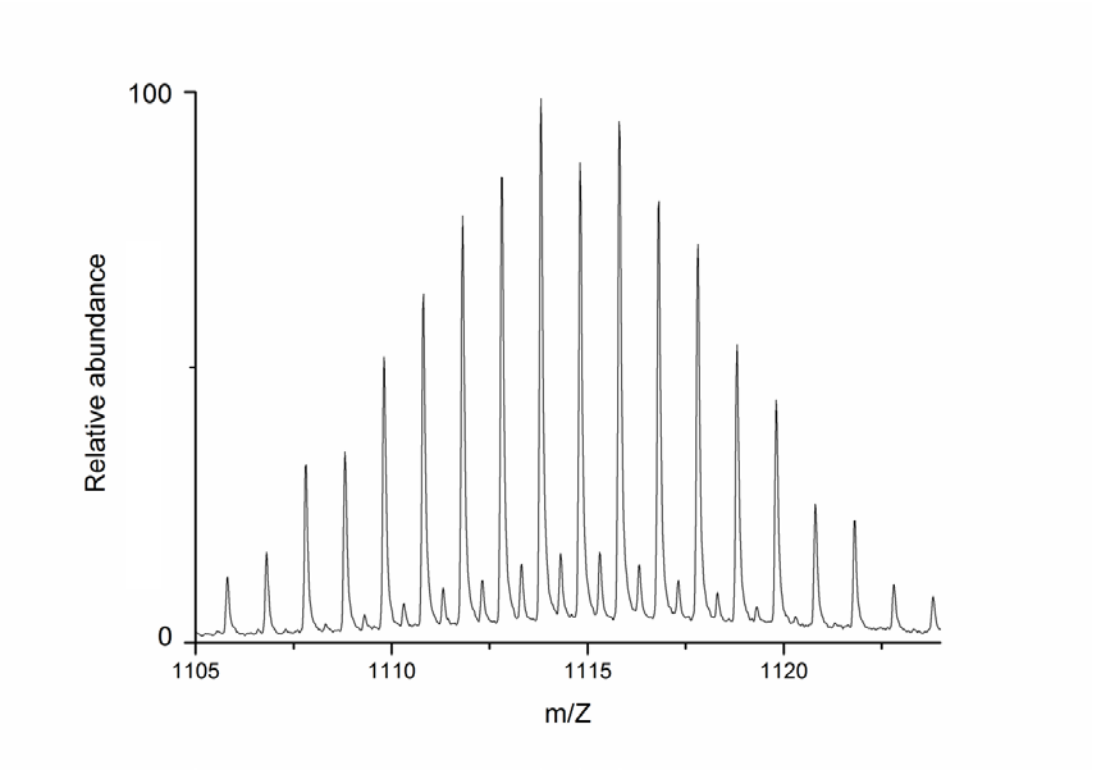

Figure S12. HRMS spectrum of **2** representing the isotopic pattern of TBA$[V_3Mo_3O_{16}(C_7H_9O_5)]^{1-}$.

Table S2. Assignment of HRMS of **2** in the negative ion mode.

Peak (m / z)	Assignment
1115 Da	TBA$[V_3Mo_3O_{16}(C_7H_9O_5)]^{1-}$
436 Da	$[V_3Mo_3O_{16}(C_7H_9O_5)]^{2-}$

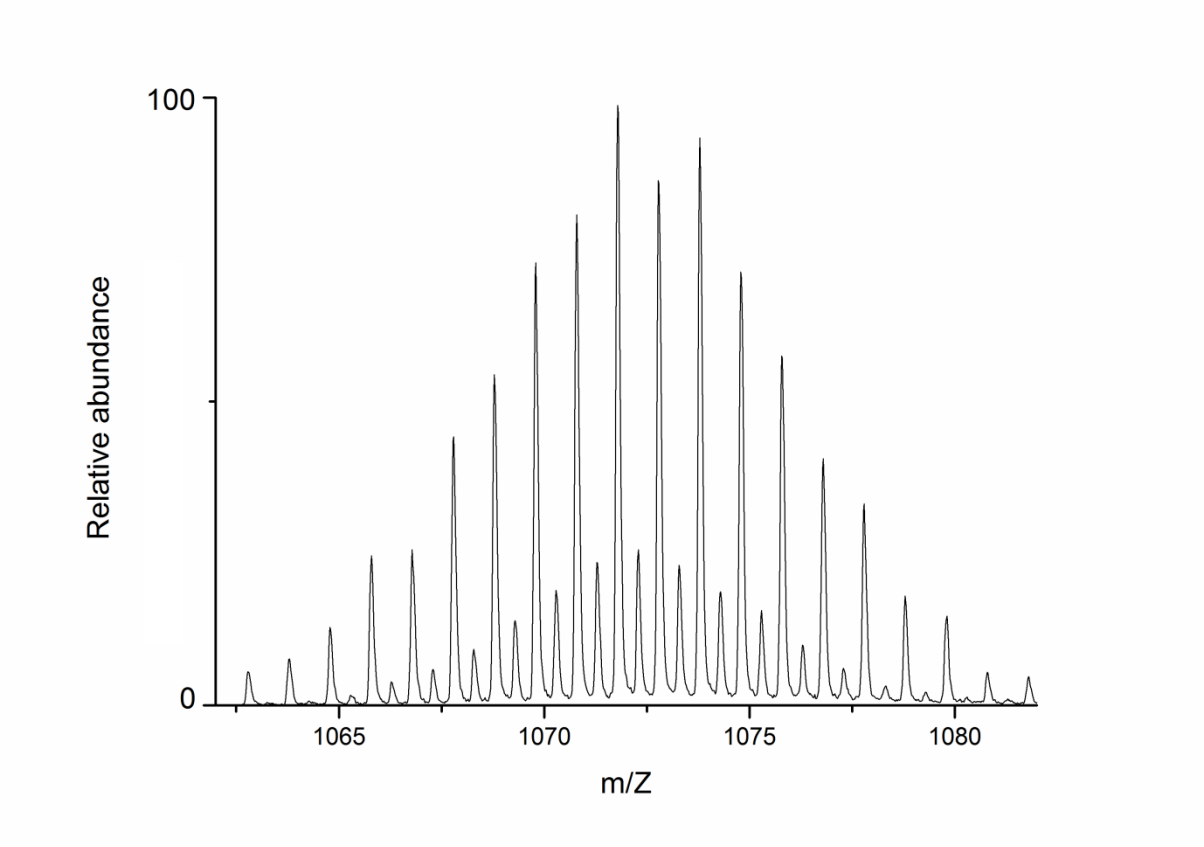

Figure S13. HRMS spectrum of **3** representing the isotopic pattern of TBA[$V_3Mo_3O_{16}(C_4H_8NO_3)$]$^{1-}$.

Table S3. Assignment of HRMS of **3** in the negative ion mode.

Peak (m / z)	Assignment
1072 Da	TBA[$V_3Mo_3O_{16}(C_4H_8NO_3)$]$^{1-}$
407 Da	[$V_3Mo_3O_{16}(C_4H_8NO_3)$]$^{2-}$

Cyclic Voltammetry

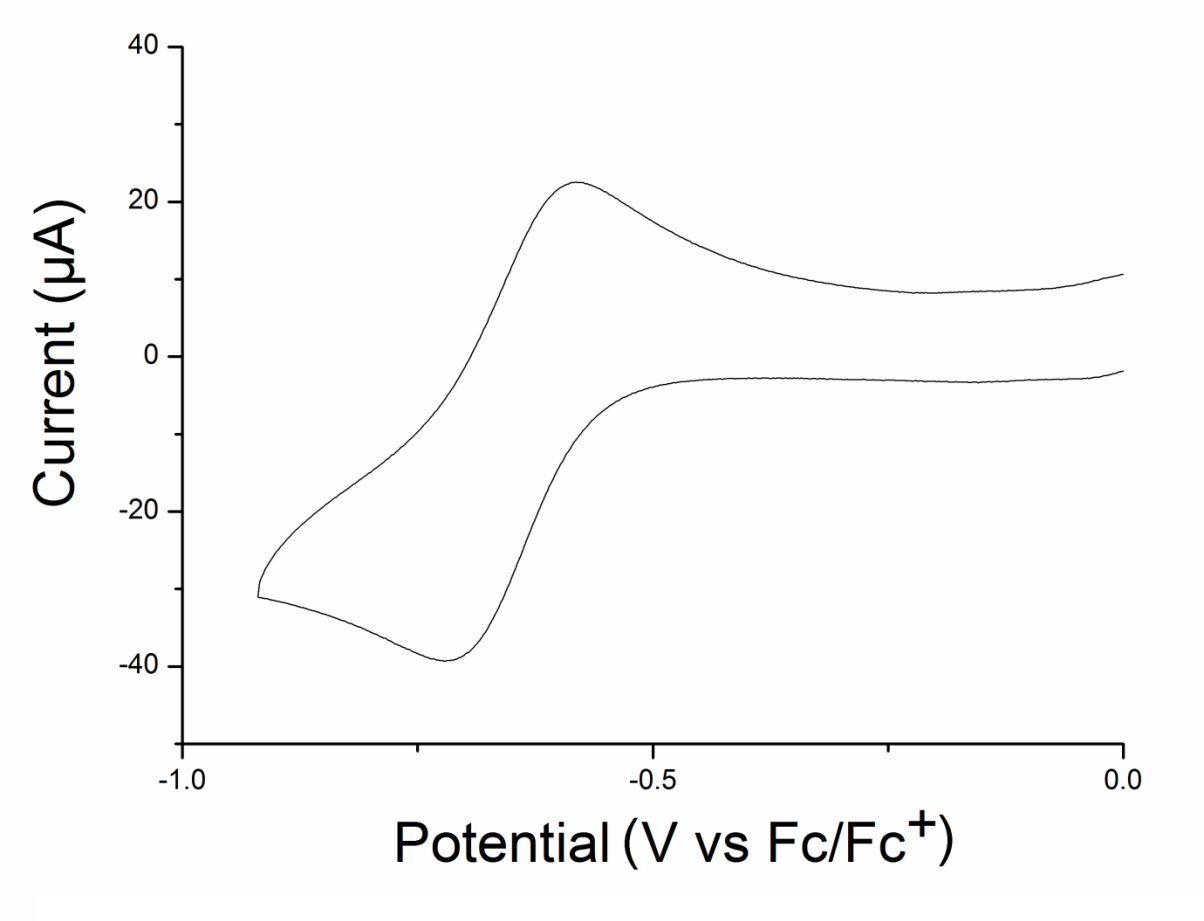

Figure S14. Cyclic Voltammogram of **1** in a 0.1 M electrolyte solution. Scan conducted at 100 mV/s. E_{pc} = -0.67 V; E_{pa} = -0.58V

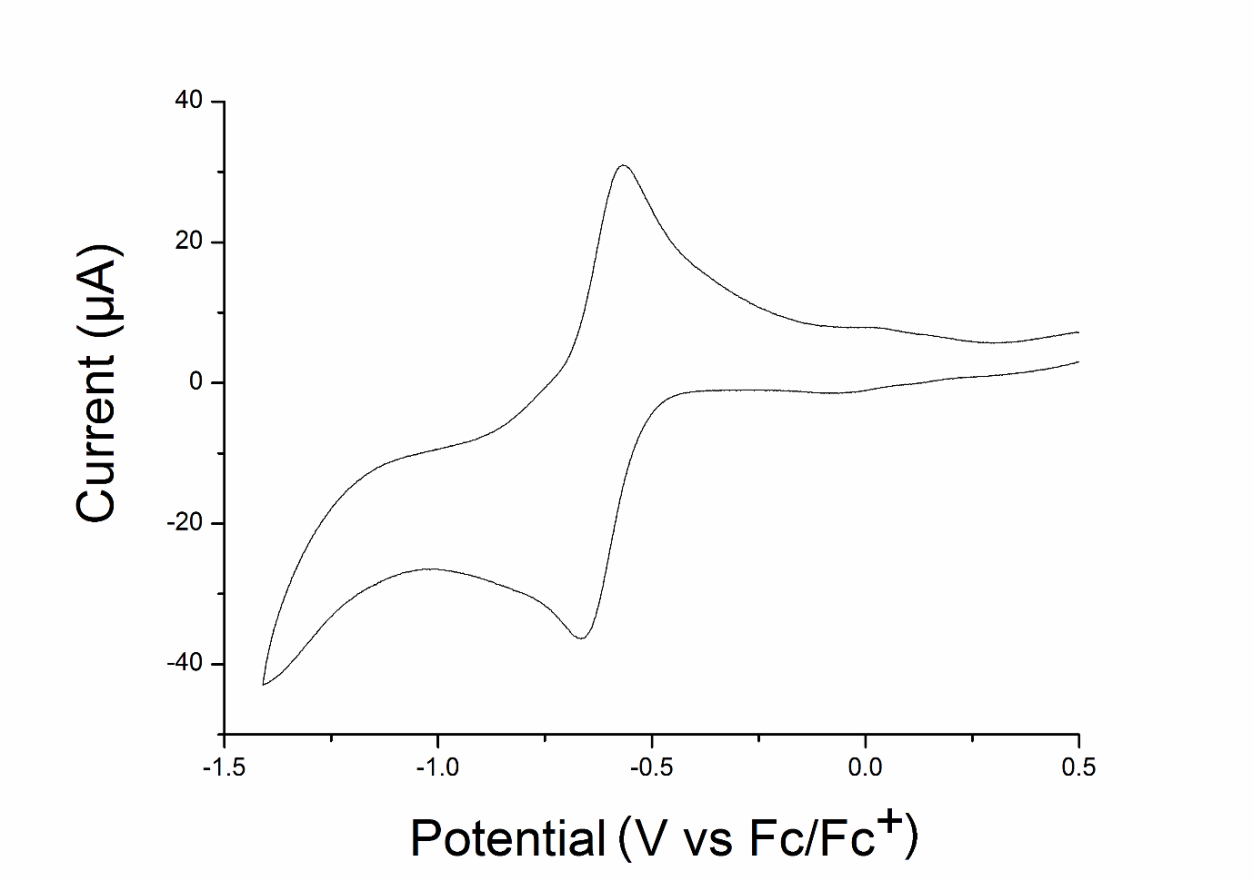

Figure S15. Cyclic Voltammogram of **2** in a 0.1 M electrolyte solution. Scans conducted at 100 mV/s. E_{pc} = -0.65 V; E_{pa} = -0.57 V.

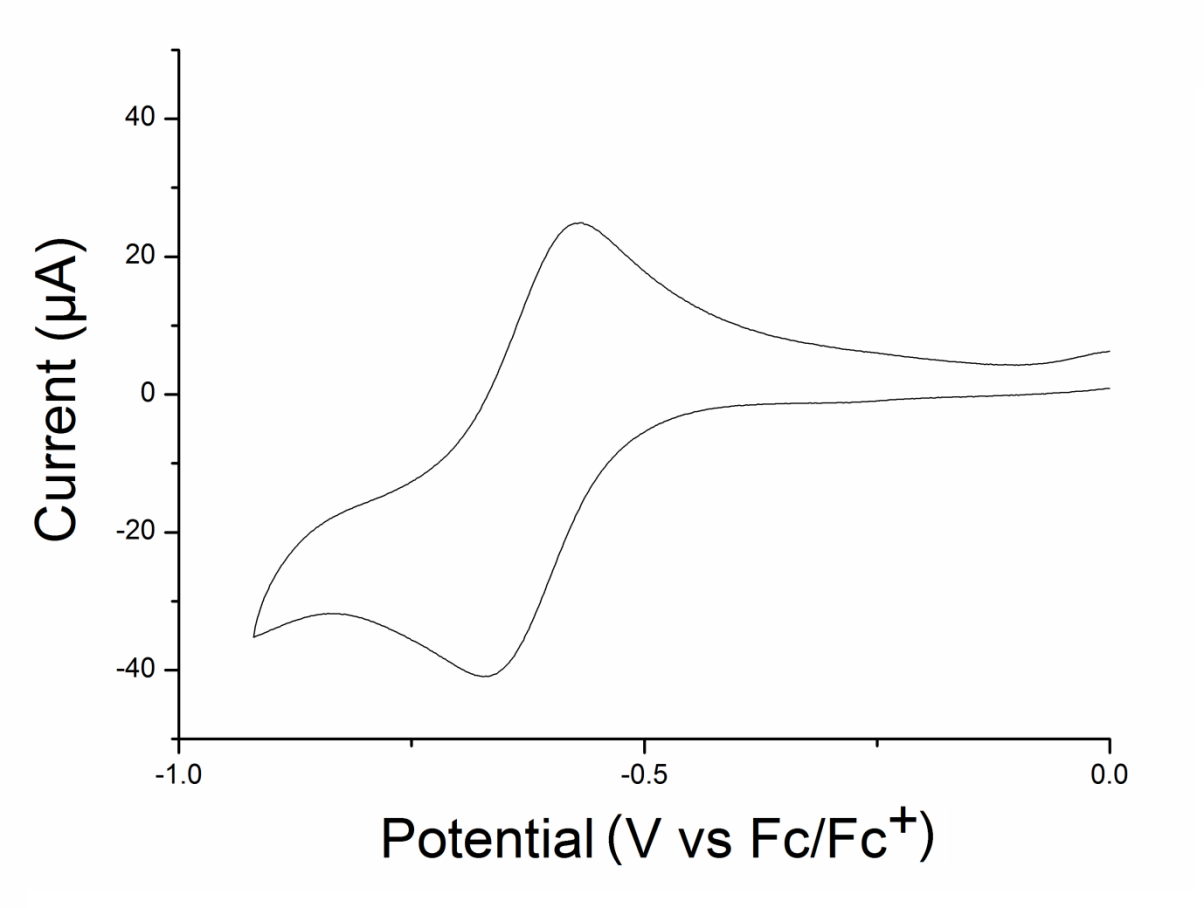

Figure S16. Cyclic Voltammogram of **3** in a 0.1 M electrolyte solution. Scans conducted at 100 mV/s. E_{pc} = -0.66 V; E_{pa} = -0.57 V.

Table S4. ^{1}H NMR assignments of **1**

fac-$[Mo_3V_3O_{16}(L)]^{2-}$ **(Isomer A)**		fac-$[Mo_3V_3O_{16}(L)]^{2-}$ **(Isomer B)**		mer-$[Mo_3V_3O_{16}(L)]^{2-}$ **(Isomer C)**	
peak	δv	peak	δv	peak	δv
$((CH_2)_3$-C-C**H$_2$**-OH	3.28 (s)	$((CH_2)_3$-C-C**H$_2$**-OH	3.39 (s)	$((CH_2)_3$-C-C**H$_2$**-OH	3.30(s)
$((CH_2)_3$-C-CH_2-OH	5.18(s)	$((CH_2)_3$-C-CH_2-OH	4.80(s)	$((CH_2)_3$-C-CH_2-OH	4.85(o)
		$((CH_2)_3$-C-CH_2-OH	4.83-4.86 (d)	$((CH_2)_3$-C-CH_2-OH	4.94-4.97 (dd)
		$((CH_2)_3$-C-CH_2-OH	5.03-5.06 (d)	$((CH_2)_3$-C-CH_2-OH	4.99-5.00 (dd)
		$((CH_2)_3$-C-CH_2-OH	5.12 (s)	$((CH_2)_3$-C-CH_2-OH	5.01-5.02(dd)
				$((CH_2)_3$-C-CH_2-OH	5.14(o)

Where: s = singlet; d = doublet; dd = doublet of doublets; o = obscured.

Table S5. ^{1}H NMR assignments of **2**

fac-$[Mo_3V_3O_{16}(L)]^{2-}$ **(Isomer A)**		fac-$[Mo_3V_3O_{16}(L)]^{2-}$ **(Isomer B)**		mer-$[Mo_3V_3O_{16}(L)]^{2-}$ **(Isomer C)**	
peak	δv	peak	δv	peak	δv
$((CH_2)_3$-C-CH_2-O-C=O-C**H$_3$**	3.01 (s)	$((CH_2)_3$-C-CH_2-O-C=O-C**H$_3$**	2.96 (s)	$((CH_2)_3$-C-CH_2-O-C=O-C**H$_3$**	2.83 (s)
$((CH_2)_3$-C-C**H$_2$**-O-C=O-CH_3	4.02 (s)	$((CH_2)_3$-C-C**H$_2$**-O-C=O-CH_3	3.90 (s)	$((CH_2)_3$-C-C**H$_2$**-O-C=O-CH_3	3.91 (S)
$((C$**H$_2$**$)_3$-C-CH_2-O-C=O-CH_3	5.20 (s)	$((C$**H$_2$**$)_3$-C-CH_2-O-C=O-CH_3	4.83-4.86 (o)	$((C$**H$_2$**$)_3$-C-CH_2-O-C=O-CH_3	4.89 (o)
		$((C$**H$_2$**$)_3$-C-CH_2-O-C=O-CH_3	5.05 (s)	$((C$**H$_2$**$)_3$-C-CH_2-O-C=O-CH_3	4.96-4.97 (dd)
		$((C$**H$_2$**$)_3$-C-CH_2-O-C=O-CH_3	5.08 (s)	$((C$**H$_2$**$)_3$-C-CH_2-O-C=O-CH_3	4.99-5.00 (dd)
		$((C$**H$_2$**$)_3$-C-CH_2-O-C=O-CH_3	5.14 (s)	$((C$**H$_2$**$)_3$-C-CH_2-O-C=O-CH_3	5.03-5.04 (dd)
				$((C$**H$_2$**$)_3$-C-CH_2-O-C=O-CH_3	5.06-5.07 (dd)
				$((C$**H$_2$**$)_3$-C-CH_2-O-C=O-CH_3	5.16-5.17 (dd)

Where: s = singlet; d = doublet; dd = doublet of doublets; o = obscured.

Table S6. ^{1}H NMR assignments of **3**

fac-$[Mo_3V_3O_{16}(L)]^{2-}$ **(Isomer A)**		fac-$[Mo_3V_3O_{16}(L)]^{2-}$ **(Isomer B)**		mer-$[Mo_3V_3O_{16}(L)]^{2-}$ **(Isomer C)**	
peak	δv	peak	δv	peak	δv
$((CH_2)_3$-C-NH_2	4.96(s)	$((CH_2)_3$-C-NH_2	4.60-4.62(d)	$((CH_2)_3$-C-NH_2	4.53(o)
		$((CH_2)_3$-C-NH_2	4.79-4.83 (d)	$((CH_2)_3$-C-NH_2	4.57-4.58(o)
		$((CH_2)_3$-C-NH_2	4.90 (s)	$((CH_2)_3$-C-NH_2	4.65-4.67 (o)
				$((CH_2)_3$-C-NH_2	4.72-4.73(d)
				$((CH_2)_3$-C-NH_2	4.74-4.75(d)
				$((CH_2)_3$-C-NH_2	4.93-4.94 (d)

Where: bs = broad singlet; s = singlet; d = doublet; dd = doublet of doublets; o = obscured.

Table S7. Crystallographic data for **1**, **2** and **3**

	1	**2**	**3**
Empirical formula	$C_{37}H_{81}N_2V_3Mo_3O_{20}$	$C_{39}H_{83}N_2V_3Mo_3O_{21}$	$C_{36}H_{80}N_3V_3Mo_3O_{19}$
Formula weight	1314.68	1354.70	1299.67
Crystal system	Monoclinic	Triclinic	Monoclinic
a / Å	15.7895(2)	21.4889(13)	15.7948(3)
b / Å	18.8620(3)	22.7196(17)	18.5129(3)
c / Å	18.1257(2)	24.1556(17)	18.2430(3)
α / °		90.952 (6)	
β / °	98.459(1)	93.807(5)	100.088(2)
γ / °		91.862(5)	
V / Å^3	5339.50(12)	11758.9(14)	5251.92 (16)
ρ g / cm^{-3}	1.686	1.533	1.694
Z	4	8	4
μ (Cu) mm^{-1}	10.447	9.497	10.605
Total reflections	22122	43456	32619
Unique reflections	10668	24359	10711
No. parameters	634	918	622
F(000)	2776	5552	2740
R_1	0.0306	0.1501	0.0693
wR_2	0.0804	0.3839	0.2428
GOF	1.028	1.281	1.157

Compound **2** displays significant crystallographic disorder, not only in terms of the structural isomerisation of the V and Mo metal centres within the polyanions, but also of the charge balancing tetrabutylammonium (TBA) cations. Refinement of the V and Mo occupancies are fixed (**Site A** 0.75 : 0.25, **Site B** 0.5 : 0.5 and **Site C** 0.25 : 0.75) based on NMR, Mass spectroscopy and elemental analysis data on a bulk sample. This formulation is consistent with that observed for **1** and **3**. A dominant orientation of the tris ligand grafted to **2** was also identified and crystallographically constrained using DFIX and DANG commands. Attempts to model the highly disordered TBA cations were unsuccessful and overcome by using a solvent mask.

Packing Diagrams

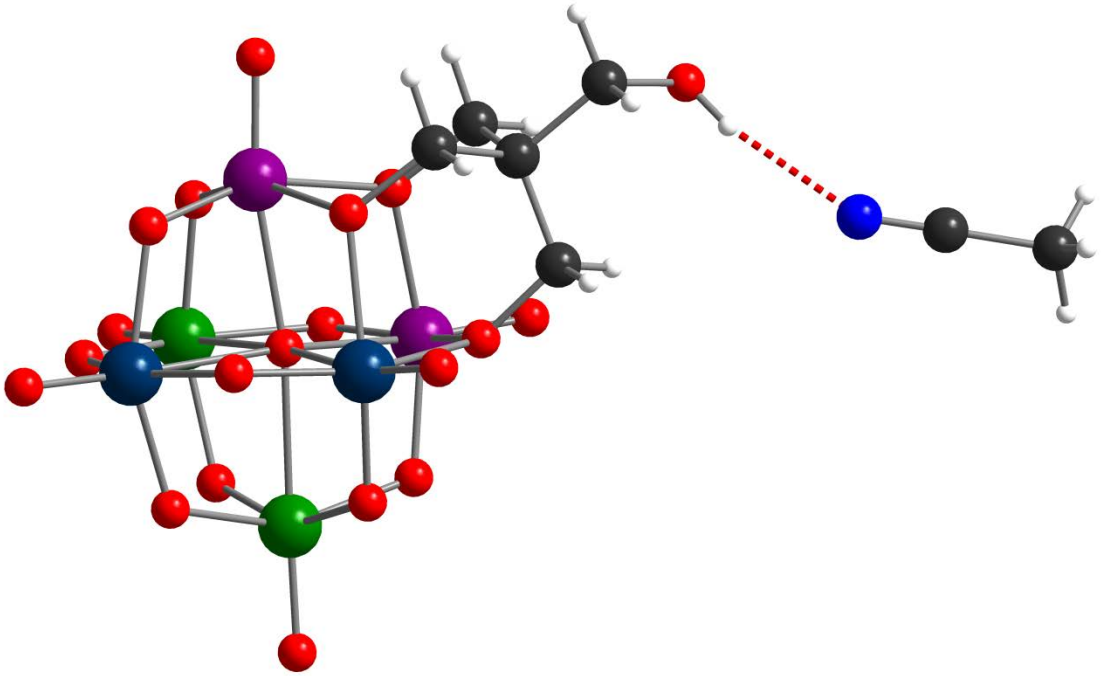

Figure S17. Intermolecular hydrogen bonding between the nitrogen from MeCN and the protons from the terminal alcohol in **1**.

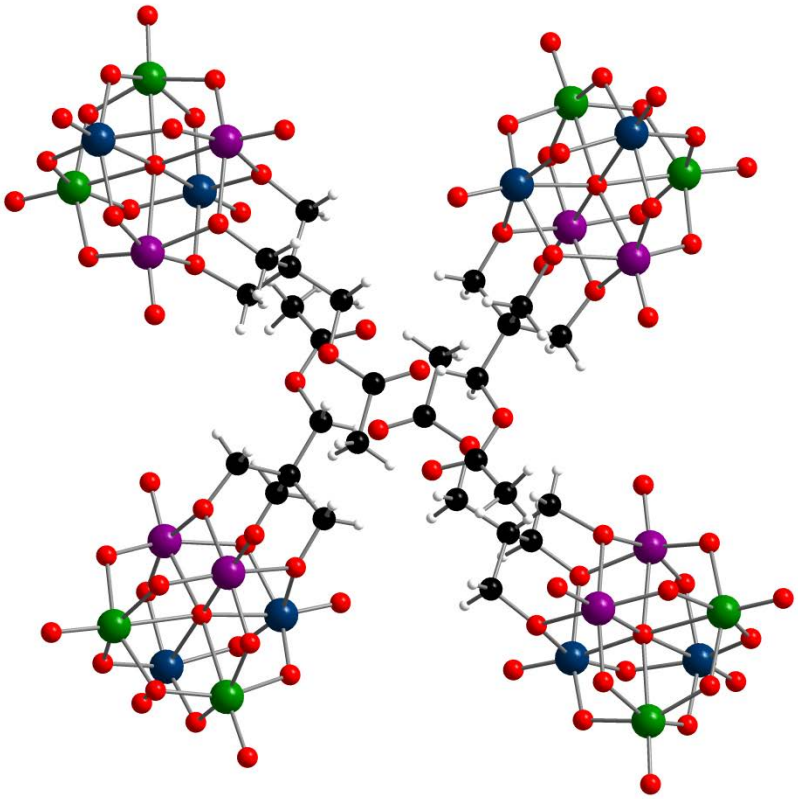

Figure S18. Intermolecular interactions between the organic ligands of **2** to form supramolecular tetramers.

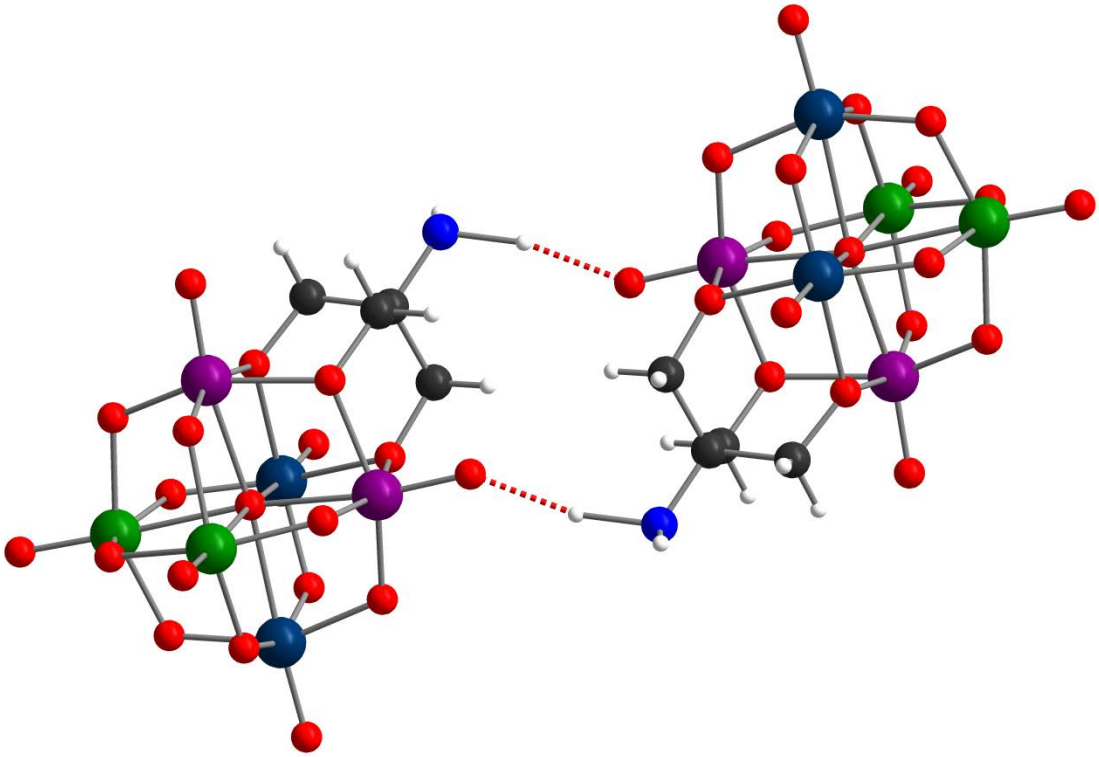

Figure S19. Intermolecular hydrogen bonded dimers between an amine proton and a site A terminal oxo ligand in **3**.

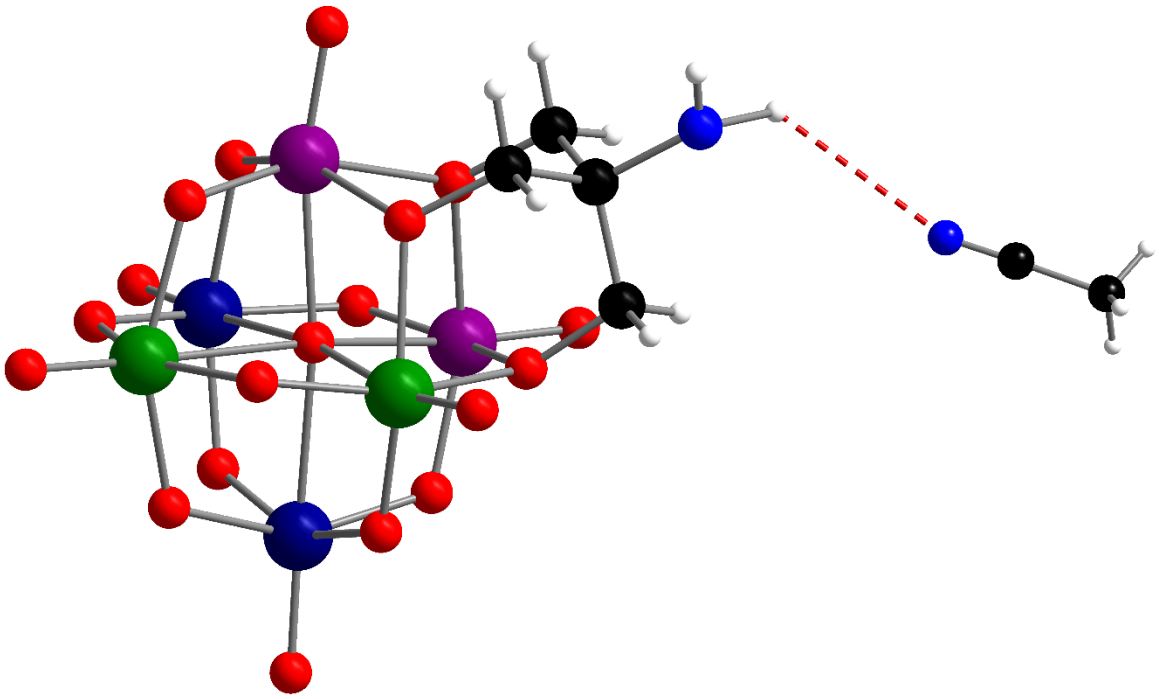

Figure S20. Intermolecular hydrogen bonding between the nitrogen from MeCN and a proton from the terminal amine in **3**.

References

1. W. Klemperer, Inorg. Synth., **2007**, 27, 74–85.
2. Sheldrick, G. M., *Acta. Cryst. Sec. A.*, **2015**, A71, 3-8.
3. Dolomanov, O. V., Bourhis, L. J., Gildea, R. J., Howard, J. A. K. and Puschmann, H., *J. Appl. Cryst.* **2009**, 42, 339-341.
4. Borg, S. J., Best, S. P., J. Electroanalytical Chem., **2002**, 535, 57-64.
5. Robert A. Scott, Charles M. Lukehart, Applications of Physical Methods to Inorganic and Bioinorganic Chemistry, **2007**, ISBN: 978-0-470-03217-6.